JOC Article
pubs.acs.org/joc

Computational Study of Cyclopropanation Reactions with Halodiazoacetates

Hanne Therese Bonge and Tore Hansen*

University of Oslo, Department of Chemistry, Sem Sælands vei 26, N-0315 Oslo, Norway

tore.hansen@kjemi.uio.no

Received January 22, 2010

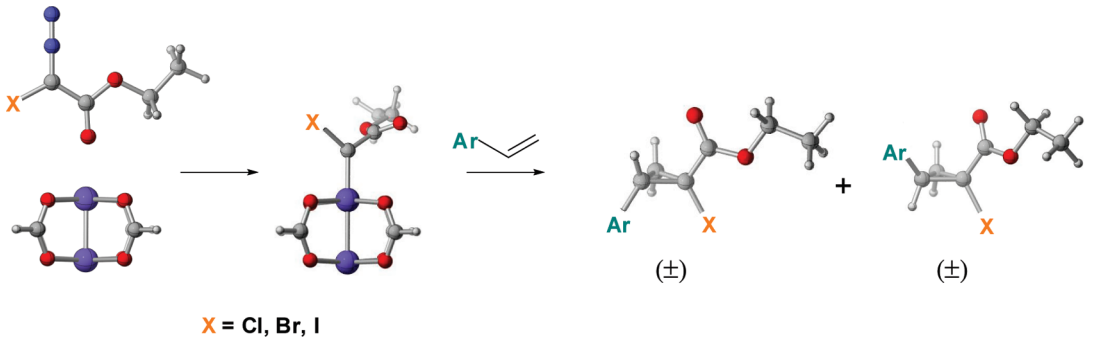

The mechanism of rhodium(II)-catalyzed cyclopropanation reactions with ethyl bromo-, chloro-, and iododiazoacetate has been studied with density functional theory calculations. The halodiazoacetates were shown to be remarkably kinetically active compared to ethyl diazoacetate, as demonstrated experimentally in a study of reaction rates and supported by the calculated low potential energy barriers for the rate-determining loss of dinitrogen. In the rhodium carbenoids formed from the halodiazoacetates, π-interactions between the halogen, the carbenoid carbon, and one rhodium atom were found. These interactions provide an explanation for the relatively high stability of these carbenoids and, consequently, the existence of small but significant potential energy barriers for the cyclopropanation step. The predicted diastereomeric ratios correspond well with the experimental results. In addition to transition states in which the alkene approaches the carbenoid in an end-on manner, as described in computational studies of cyclopropanations with other diazo compounds, side-on trajectory transition states were found to be of importance. The relative energies of the side-on trajectory transition states compared to the end-on trajectory transition states were shown to be affected by both the substrate alkene and the carbenoid substituents, a fact that should be taken into consideration when using models to explain and predict the stereochemical outcome of cyclopropanation reactions.

Introduction

The cyclopropane ring is an important moiety in organic chemistry. Endowed with a unique reactivity and a well-defined three-dimensional structure, the smallest among the carbocycles is frequently employed both in synthesis[1−4] and as a motif in pharmaceuticals[5] and natural products.[6] The methods for synthesis of cyclopropanes are therefore plentiful.[7−9] One protocol, however, has a particularly widespread application: transition-metal-catalyzed decomposition of diazo compounds in the presence of olefins.[10] The intermediacy of a metal

(1) Rubin, M.; Rubina, M.; Gevorgyan, V. *Chem. Rev.* **2007**, *107*, 3117.
(2) de Meijere, A.; Kozhushkov, S. I.; Hadjiarapoglou, L. P. *Small Ring Compd Org. Synth. VI* **2000**, *207*, 149.
(3) de Meijere, A.; Kozhushkov, S. I.; Khlebnikov, A. F. *Small Ring Compd Org. Synth. VI* **2000**, *207*, 89.
(4) Iwasawa, N.; Narasaka, K. *Small Ring Compd Org. Synth. VI* **2000**, *207*, 69.
(5) Salaün, J. *Small Ring Compd Org. Synth. VI* **2000**, *207*, 1.
(6) Halton, B. *Chem. N. Z.* **2007**, *71*, 155.
(7) Salaün, J. *Chem. Rev.* **1989**, *89*, 1247.
(8) Donaldson, W. A. *Tetrahedron* **2001**, *57*, 8589.
(9) Pellissier, H. *Tetrahedron* **2008**, *64*, 7041.
(10) Doyle, M. P.; McKervey, M. A.; Ye, T. *Modern Catalytic Methods for Organic Synthesis with Diazo Compounds: From Cyclopropanes to Ylides*; Wiley: New York, 1998,

DOI: 10.1021/jo100113b Published on Web 03/10/2010

SCHEME 1. Synthesis of Ethyl Halodiazoacetates and Subsequent Cyclopropanation

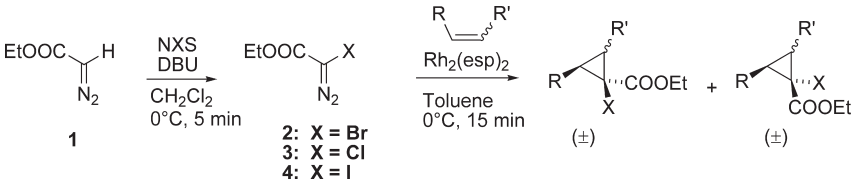

carbenoid, less reactive than a free carbene, enables reactions of good chemo-, regio-, and stereoselectivity while still allowing for high yields. A cardinal position is held by the electrophilic carbenoids, a group of highly versatile intermediates whose frequent areas of use also include C−H insertion and generation of ylides, and that has found wide application in the synthesis of functionalized cyclopropanes.[11−14] Generated from diazo compounds with one or two electron-withdrawing (acceptor) substituents on the carbene carbon, they have been dubbed acceptor-, donor/acceptor-, or acceptor/acceptor-substituted carbenoids depending on these substituents.

We have lately been focusing our work on halodiazoacetates, a synthetically interesting group of halogenated diazo compounds.[15,16] Ethyl bromo-, chloro-, and iododiazoacetate (**2**, **3**, and **4**, Scheme 1) are readily available using our previously described protocol,[15] by which quantitative formation of the halodiazoacetates is achieved through treatment of commercially available ethyl diazoacetate (EDA, **1**) with DBU and the appropriate *N*-halosuccinimide. We have explored the use of ethyl halodiazoacetates in both Rh(II)-catalyzed C−H insertion reactions[16] and cyclopropanation reactions.[15] In intermolecular Rh(II)-catalyzed cyclopropanation reactions with electron-rich, sterically unencumbered alkenes, the halodiazoacetates give good to excellent yields of halocyclopropanes. Reaction with 1,1-diphenylethene proceeds well, but the more sterically hindered 1,2-disubstituted *cis*- and *trans*-stilbene are unreactive. The diastereomeric ratio of the product cyclopropanes is typically in the area 6:1 to 9:1, favoring the diastereomer with the ester functionality in a *trans* relationship with the olefinic substituent. With *N*-vinylphthalimide as the alkene the diastereomeric ratio is higher than 20:1. Kinetically, the halodiazoacetates are highly reactive, as illustrated by reaction times of less than 15 min at room temperature, and they are not prone to dimerization under the reaction conditions. Their reactivity profile is thus quite different from that of EDA, which typically gives a diastereomeric ratio of around 2:1 and a considerable amount of byproduct formed through formal carbenoid dimerization, and also requires longer reaction times.[10]

Rh(II)-catalyzed cyclopropanation with halodiazoacetates represents a novel tool for selective introduction of halogens. Thus, expanding the knowledge about the halodiazoacetates is of interest from a synthetic point of view, as understanding more about their reactivity may shed new light on their synthetic utility. Moreover, the rhodium carbenoids formed from these halogenated diazo compounds are a new group of carbenoids whose properties have yet to be fully explored. We present herein a full computational study of the reaction mechanism for Rh(II)-catalyzed cyclopropanation with ethyl halodiazoacetates **2**−**4**, exploring the reaction steps and the nature of the intermediates. The three halodiazoacetates are compared to each other and to EDA (**1**), providing explanations for their experimentally observed reactivity. The basis for the diastereoselectivity is discussed, showing how the trajectory of the alkene in the cyclopropanation transition states can be influenced by both the substrate alkene and the carbenoid substituents.

Results and Discussion

Experimental Study of Reaction Rates. Cyclopropanations with all three ethyl halodiazoacetates **2**−**4** are rapid reactions. Vigorous evolution of N_2 gas starts immediately when the catalyst is added to the diazo compound and olefin, and the reaction is finished after only a few minutes of stirring at room temperature. To examine the cyclopropanation reaction rate more closely, experiments were conducted in which the gas evolved during the reaction was trapped. The reactions took place in toluene, with styrene as the substrate and $Rh_2(esp)_2$ as the catalyst, mirroring the standard conditions for cyclopropanations with ethyl halodiazoacetates.[15] They were performed at 0 °C with a catalyst loading of 0.5 mol %, thus slowing the rate somewhat compared to the rate at the standard conditions, in order to facilitate the recordings. Experiments were carried out with EDA (**1**) and bromodiazoacetate **2**, using identical conditions, and the amount of evolved gas was recorded as a function of time.

The results (Figure 1) show that the initial rate of cyclopropanation with halogenated diazo compound **2** is much higher than with **1**. In the reaction with **2**, 50% of the total gas volume is evolved within the first 15 s, something that takes 8 min in the reaction with **1**. This implies a lower turnover-limiting barrier in the catalytic cycle with **2** compared to **1** and sets the halodiazoacetates apart from both acceptor-substituted **1** and the donor/acceptor-substituted methyl phenyldiazoacetate, which has been shown to display similar kinetics to **1**.[18]

Computational Study

Computational Methods. Density functional theory (DFT) was employed to investigate the reaction mechanism using the Becke-3LYP hybrid functional.[19,20] The stationary structures of

(11) Davies, H. M. L.; Denton, J. R. *Chem. Soc. Rev.* **2009**, *38*, 3061.
(12) Marcoux, D.; Goudreau, S. R.; Charette, A. B. *J. Org. Chem.* **2009**, *74*, 8939.
(13) Marcoux, D.; Charette, A. B. *Angew. Chem., Int. Ed.* **2008**, *47*, 10155.
(14) Chuprakov, S.; Kwok, S. W.; Zhang, L.; Lercher, L.; Fokin, V. V. *J. Am. Chem. Soc.* **2009**, *131*, 18034.
(15) Bonge, H. T.; Pintea, B.; Hansen, T. *Org. Biomol. Chem.* **2008**, *6*, 3670.
(16) Bonge, H. T.; Hansen, T. *Synthesis* **2009**, 91.
(17) Davies, H. M. L.; Clark, T. J.; Church, L. A. *Tetrahedron Lett.* **1989**, *30*, 5057.
(18) Nowlan, D. T.; Gregg, T. M.; Davies, H. L. M.; Singleton, D. A. *J. Am. Chem. Soc.* **2003**, *125*, 15902.
(19) Becke, A. D. *J. Chem. Phys.* **1993**, *98*, 5648.
(20) Lee, C. T.; Yang, W. T.; Parr, R. G. *Phys. Rev. B* **1988**, *37*, 785.

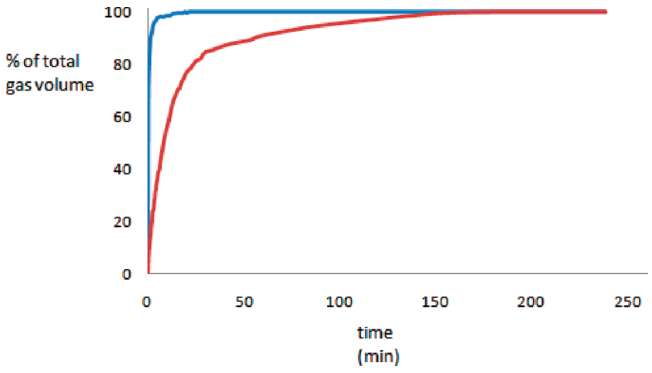

FIGURE 1. Evolution of gas as a function of time, recorded for cyclopropanation of styrene with EDA (**1**) (red line) and ethyl bromodiazoacetate (**2**) (blue line).

the potential energy surfaces were fully optimized at the B3LYP level of theory using the LANL2DZ basis set for Rh and 6-31G* for C, H, N, and O. The method and the basis sets are shown to give reliable results for other rhodium(II) carbenoids.[18,21−26] For F, Cl, Br, and I, the basis set 6-311G* was used. Basis set definition for iodine was obtained from the EMSL basis set exchange library.[27] Natural bond orbital (NBO) analyses[28−30] were performed at the same level of theory. Wiberg bond indices[31] and NBO charges were calculated from NBO theory as implemented in Gaussian 03. Stationary structures were characterized by normal coordinate analysis: No imaginary frequencies for equilibrium structures, and one imaginary frequency for transition structures. Intrinsic reaction coordinate (IRC) calculations were used to confirm that the optimized transition structures correctly connect the relevant reactants and products. The reported energies are the zero-point corrected sum of electronic and thermal energies at 25 °C, scaled according to literature (0.9806).[32] All calculations were carried out using the Gaussian 03 program package.[33] Molecular orbitals were generated using GaussView.

Chemical Models. In accordance with current theory,[10] the only mechanism studied was the Yates mechanism[34] of complexation of the negatively polarized carbon of the diazo compound to the rhodium catalyst, loss of nitrogen to generate a rhodium carbenoid, followed by cyclopropanation by the rhodium carbenoid. For the cyclopropanation step, different mechanisms have been proposed: [2 + 1] pathways initiated by either an "end-on"[18] or a "side-on"[35] approach of the alkene to the carbene-catalyst complex, or a "face-on" approach leading to a [2 + 2] cycloaddition of the alkene to the metal carbenoid, enabled by reversible dechelation of one of the ligands on rhodium.[36,37] The [2 + 2] pathway, which now has been largely disregarded in dirhodium(II) catalysis, was briefly explored, but no transition structures were located. We therefore chose to focus our efforts on a [2 + 1] pathway. Based on a kinetic study by Pirrung et al.,[38] we also assumed complexation of only one carbenoid ligand per molecule of dirhodium catalyst.

The simple dirhodium tetraformate was chosen as the catalyst. This complex has found little practical use in synthesis because of its poor solubility in organic solvents. It has, however, been successfully utilized as a model catalyst in computational studies of Rh(II)-catalyzed carbenoid reactions,[18,21−23,25] and in the interest of computational facility as well as to enable direct comparison with earlier studies, we chose to use $Rh_2(O_2CH)_4$ as a model catalyst. Cyclopropanations with halodiazoacetates **2**−**4**, and also **1** for comparison, were studied. Styrene, the simplest of the olefins previously tested experimentally in cyclopropanation reactions with the halodiazoacetates, was chosen as the standard alkene for the calculations. Since the reaction with *N*-vinylphthalimide gives a considerably higher diastereomeric ratio in cyclopropanation reactions,[15] this alkene was also studied computationally. The solvent used in the cyclopropanations with the halodiazoacetates is toluene, which has a very small dielectric constant. As for similar carbenoid reactions, the cyclopropanation reaction is expected to be affected less by solvent polarity, and more by ligation of solvent molecules, and any other ligands present, to the rhodium atoms, complicating the prediction of solvent effects. Because of this, and following precedence from earlier studies of carbenoid reactions,[18,21,23,25,39,40] no allowance was made for solvent effects.

Cyclopropanation of Styrene with Ethyl Bromodiazoacetate (2) and EDA (1). The energy profile and structures of the reaction course for $Rh_2(O_2CH)_4$-catalyzed cyclopropanation of styrene with ethyl bromodiazoacetate (**2**) are shown in Scheme 2 and Figure 2. Several rotamers and conformers were examined; the depicted structures are the stationary structures of lowest energy for each step.

The catalytic cycle for cyclopropanation of styrene with ethyl bromodiazoacetate (**2**) is instigated by interaction between **2** and $Rh_2(O_2CH)_4$, resulting in complex **5**. The complexation is predicted to be exothermic, with an 8.1 kcal/mol stabilization energy. Nitrogen extrusion from complex **5** is the rate limiting step of the catalytic cycle; transition state **TS-6** represents a predicted barrier of 8.0 kcal/mol. The loss of nitrogen results in

(21) Nakamura, E.; Yoshikai, N.; Yamanaka, M. *J. Am. Chem. Soc.* **2002**, *124*, 7181.
(22) Howell, J. A. S. *Dalton Trans.* **2007**, 1104.
(23) Yoshikai, N.; Nakamura, E. *Adv. Synth. Catal.* **2003**, *345*, 1159.
(24) Sheehan, S. M.; Padwa, A.; Snyder, J. P. *Tetrahedron Lett.* **1998**, *39*, 949.
(25) Padwa, A.; Snyder, J. P.; Curtis, E. A.; Sheehan, S. M.; Worsencroft, K. J.; Kappe, C. O. *J. Am. Chem. Soc.* **2000**, *122*, 8155.
(26) Others have also been successfully used; see refs 39 and 40.
(27) Schuchardt, K. L.; Didier, B. T.; Elsethagen, T.; Sun, L. S.; Gurumoorthi, V.; Chase, J.; Li, J.; Windus, T. L. *J. Chem. Inf. Model.* **2007**, *47*, 1045.
(28) Reed, A. E.; Weinstock, R. B.; Weinhold, F. *J. Chem. Phys.* **1985**, *83*, 735.
(29) Reed, A. E.; Curtiss, L. A.; Weinhold, F. *Chem. Rev.* **1988**, *88*, 899.
(30) *NBO version 3.1*: Glendening, E. D., Reed, A. E., Carpenter, J. E., Weinhold, F. University of Wisconsin: Madison, WI, 1990
(31) Wiberg, K. B. *Tetrahedron* **1968**, *24*, 1083.
(32) Scott, A. P.; Radom, L. *J. Phys. Chem.* **1996**, *100*, 16502.
(33) Frisch, M. J., Trucks, G. W.; Schlegel, H. B.; Scuseria, G. E.; Robb, M. A.; Cheeseman, J. R.; Montgomery, J. A., Jr.; Vreven, T.; Kudin, K. N.; Burant, J. C.; Millam, J. M.; Iyengar, S. S.; Tomasi, J.; Barone, V.; Mennucci, B.; Cossi, M.; Scalmani, G.; Rega, N.; Petersson, G. A.; Nakatsuji, H.; Hada, M.; Ehara, M.; Toyota, K.; Fukuda, R.; Hasegawa, J.; Ishida, M.; Nakajima, T.; Honda, Y.; Kitao, O.; Nakai, H.; Klene, M.; Li, X.; Knox, J. E.; Hratchian, H. P.; Cross, J. B.; Bakken, V.; Adamo, C.; Jaramillo, J.; Gomperts, R.; Stratmann, R. E.; Yazyev, O.; Austin, A. J.; Cammi, R.; Pomelli, C.; Ochterski, J. W.; Ayala, P. Y.; Morokuma, K.; Voth, G. A.; Salvador, P.; Dannenberg, J. J.; Zakrzewski, V. G.; Dapprich, S.; Daniels, A. D.; Strain, M. C.; Farkas, O.; Malick, D. K.; Rabuck, A. D.; Raghavachari, K.; Foresman, J. B.; Ortiz, J. V.; Cui, Q.; Baboul, A. G.; Clifford, S.; Cioslowski, J.; Stefanov, B. B.; Liu, G.; Liashenko, A.; Piskorz, P.; Komaromi, I.; Martin, R. L.; Fox, D. J.; Keith, T.;. Al-Laham, M. A.; Peng, C. Y.; Nanayakkara, A.; Challacombe, M.; Gill, P. M. W.; Johnson, B.; Chen, W.; Wong, M. W.; Gonzalez, C.; Pople, J. A. *Gaussian 03, Revision D.02*, Gaussian, Inc., Wallingford CT, 2004.
(34) Yates, P. *J. Am. Chem. Soc.* **1952**, *74*, 5376.
(35) Davies, H. M. L.; Bruzinski, P. R.; Lake, D. H.; Kong, N.; Fall, M. J. *J. Am. Chem. Soc.* **1996**, *118*, 6897.
(36) Lou, Y.; Horikawa, M.; Kloster, R. A.; Hawryluk, N. A.; Corey, E. J. *J. Am. Chem. Soc.* **2004**, *126*, 8916.
(37) Lou, Y.; Remarchuk, T. P.; Corey, E. J. *J. Am. Chem. Soc.* **2005**, *127*, 14223.
(38) Pirrung, M. C.; Morehead, A. T. *J. Am. Chem. Soc.* **1996**, *118*, 8162.
(39) Hansen, J.; Autschbach, J.; Davies, H. M. L. *J. Org. Chem.* **2009**, *74*, 6555.
(40) Hansen, J.; Li, B.; Dikarev, E.; Autschbach, J.; Davies, H. M. L. *J. Org. Chem.* **2009**, *74*, 6564.

SCHEME 2. Calculated Pathway for $Rh_2(O_2CH)_4$-Catalyzed Cyclopropanation of Styrene with Ethyl Bromodiazoacetate (2)[a]

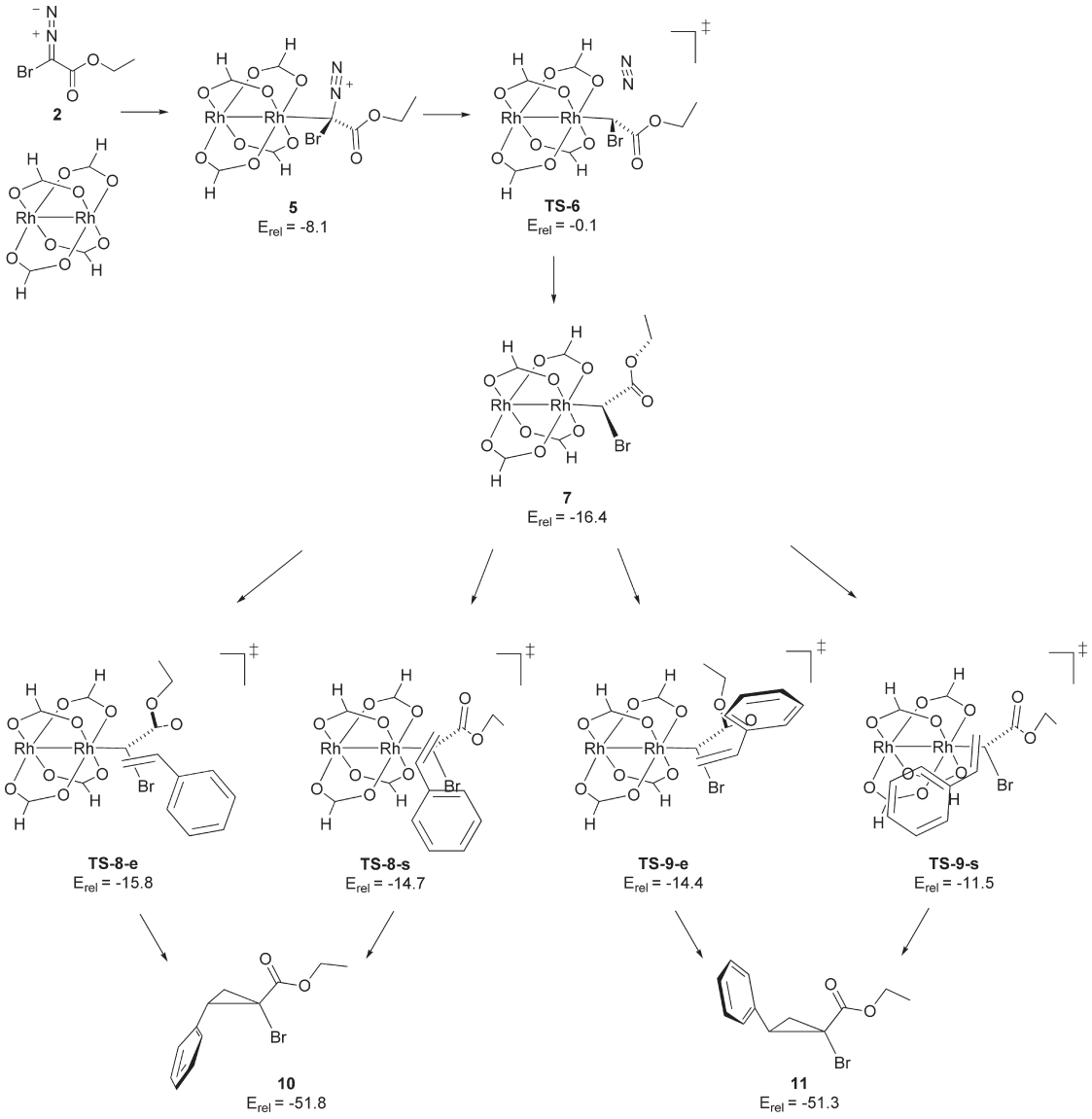

[a]Structures are shown in the Supporting Information.

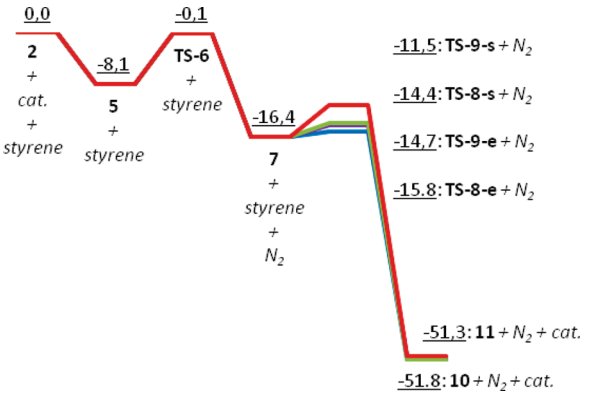

FIGURE 2. Energy profile for $Rh_2(O_2CH)_4$-catalyzed cyclopropanation of styrene with ethyl bromodiazoacetate (**2**).

formation of rhodium carbenoid **7**. The formation of **7** is quite exothermic, **7** being 8.2 kcal/mol more stable than complex **5**, and can be considered irreversible. The following cyclopropanation reaction between the rhodium carbenoid and styrene takes place in a single step; no intermediates were localized along the intrinsic reaction coordinate. There are two pairs of diastereomeric transition states leading to the two diastereomeric cyclopropane products **10** and **11**, as styrene can approach the carbenoid complex through either an end-on trajectory, the alkene parallel to the rhodium−carbon bond, or a side-on trajectory, with the alkene perpendicular. End-on trajectory transition state **TS-8-e** and side-on trajectory transition state **TS-8-s**, the transition states leading to the *Z*-substituted cyclopropane (**10**, in which the bromine and the phenyl group are *cis* to each other), represent predicted barriers of 0.7 and 1.8 kcal/mol, respectively, whereas transition state **TS-9-e**, leading to the *E*-substituted cyclopropane (**11**), represents a barrier of 2.0 kcal/mol. Side-on trajectory transition state **TS-9-s** represents a barrier of 4.9 kcal/mol and is thus not of importance. From the transition states follow downhill paths to the diastereomeric cyclopropanes and the regenerated catalyst. The cyclopropanation step is, for both diastereomers, a

SCHEME 3. Calculated Pathway for $Rh_2(O_2CH)_4$-Catalyzed Cyclopropanation of Styrene with EDA (1)

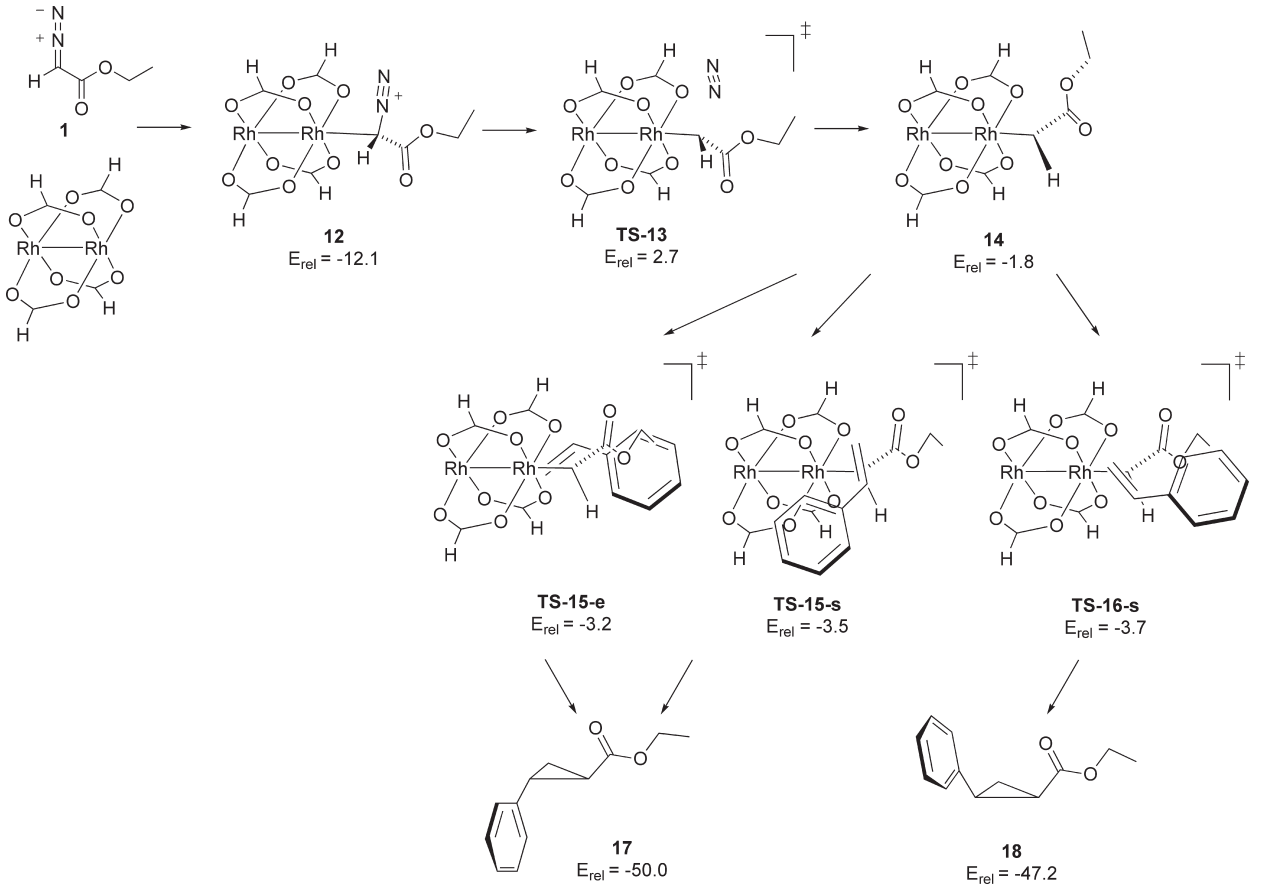

highly exothermic step, evident by a predicted stabilization energy of more than 30 kcal/mol compared to carbenoid complex **7**. Relative to the starting materials (**2**, styrene and $Rh_2(O_2CH)_4$), cyclopropane **10** is 51.8 kcal/mol lower in energy, 51.3 kcal/mol for **11**.

The corresponding results for EDA (**1**) are shown in Scheme 3 and Figure 3. Nowlan et al. have studied the cyclopropanation of styrene with methyl diazoacetate and report that no potential energy saddle point could be found for the cyclopropanation step in this reaction.[41] We did, however, identify transition states leading to both of the diastereomeric cyclopropanes **17** and **18**. With the alkene rather strongly tilted relative to the axes parallel or perpendicular to the Rh−C bond, we found one end-on and one side-on-like trajectory transition state giving **17** (**TS-15-e** and **TS-17-s**) and one end-on-like giving **18** (**TS-16-s**).

The diazo compound−catalyst complex is more stable than the corresponding free diazo compound and catalyst for both **1** and **2**. As $Rh_2(O_2CH)_4$ complexes the diazo compound, it is activated for nitrogen extrusion: The C−N bond in **2** is lengthened (1.303 → 1.365 Å) and the N−N bond shortened (1.141 → 1.122 Å) upon complexation. The same is observed for the complexation of **1**, although to a somewhat lower degree. The nitrogen extrusion step is the rate-determining step of the catalytic cycle for both of the studied cyclopropanation reactions. Nitrogen extrusion from complex **12** formed from EDA (**1**) and $Rh_2(O_2CH)_4$ has a calculated barrier of 14.8 kcal/mol.

For complex **5**, formed from ethyl bromodiazoacetate (**2**) and $Rh_2(O_2CH)_4$, the corresponding barrier is much lower, only 8.0 kcal/mol. As Pirrung et al. have demonstrated,[42] the rates of Rh(II)-catalyzed reactions with diazo compounds can be decreased by nonproductive complexation of reactants to the catalyst. This was shown to be the case for methyl vinyldiazoaceate,[18] for which the initial calculated barrier of 11.7 kcal/mol for nitrogen extrusion was too low to explain the experimental observations of K_m's and rates very similar to those of **1**. When reversible formation of other, more stable diazo compound-catalyst complexes was taken into account, lower K_m's and rates were predicted, corresponding well with the experimental results. We therefore searched for any alternative, bystander

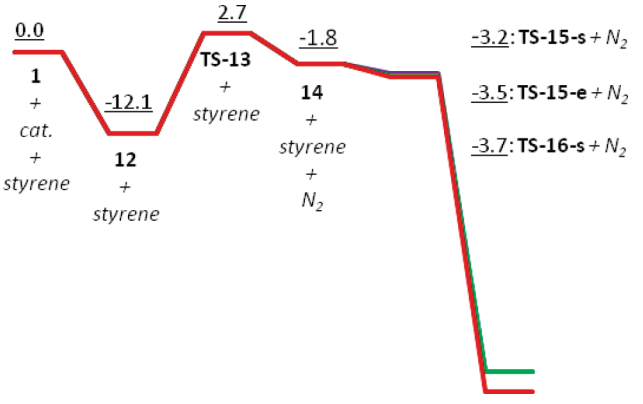

FIGURE 3. Energy profile for $Rh_2(O_2CH)_4$-catalyzed cyclopropanation of styrene with EDA (**1**).

(41) An approximate end-on trajectory transition state was reported, lower in energy than the carbenoid complex.

(42) Pirrung, M. C.; Liu, H.; Morehead, A. T. *J. Am. Chem. Soc.* **2002**, *124*, 1014.

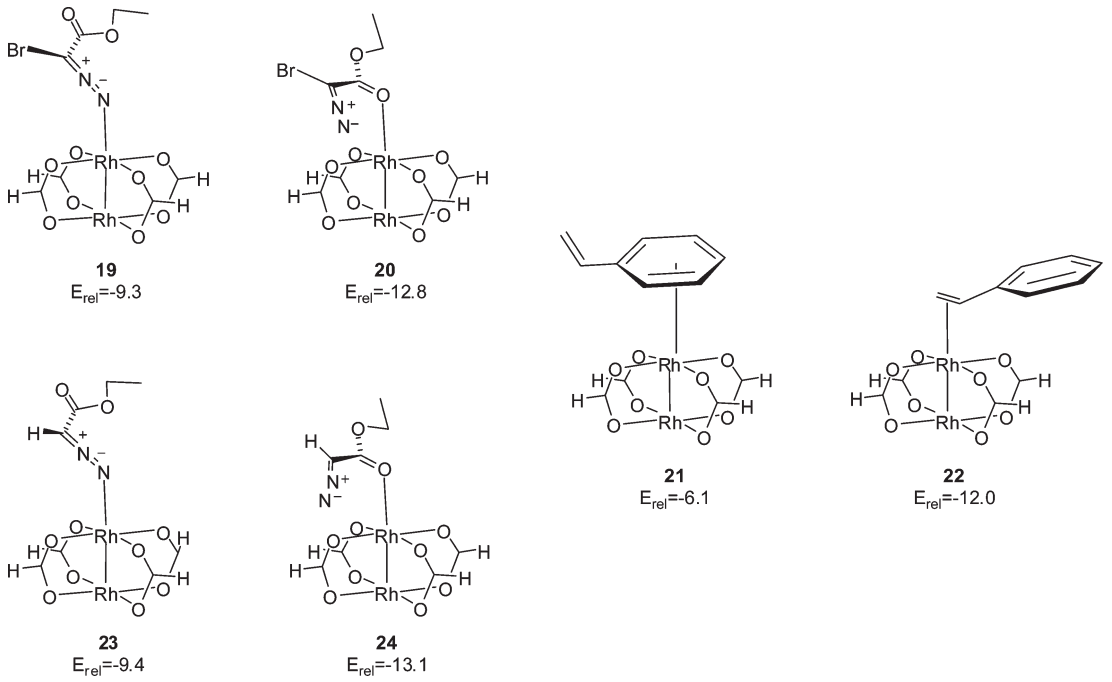

FIGURE 4. Bystander complexes formed between $Rh_2(O_2CH)_4$ and compounds **1**, **2**, or styrene.

complexes between $Rh_2(O_2CH)_4$ and either the diazo compound or styrene to see whether such complexes might be important in our case as well.

For brominated diazo compound **2**, complexes **19** and **20** (Figure 4) were identified in which **2** coordinate to $Rh_2(O_2CH)_4$ through the terminal nitrogen of the diazo group or through the carbonyl oxygen, respectively. Both **19** and **20** are more stable relative to their precursors than is **5**; whereas product-forming complex **5** has a relative energy of −8.1 kcal/mol, the relative energies of bystander complexes **19** and **20** are −9.3 and −12.8 kcal/mol, respectively. For styrene, complexes **21** and **22** were found. Complex **21**, in which styrene is coordinated via the aromatic ring, is less stable than **5**, with a relative energy of −6.1 kcal/mol. Complex **22**, on the other hand, has styrene coordinated via the alkene moiety and a relative energy of −12.0 kcal/mol. The existence of more stable complexes, even if they just are bystanders to the reaction pathway, will affect the rate of the total cyclopropanation reaction by lowering the overall initial energy of the system. Following the reasoning of Nowlan et al.,[18] assuming that the height of the energy barrier for loss of nitrogen is governed by the energy difference between the more stable complex **20** and transition state **TS-6**, a new energy barrier of 12.7 kcal/mol results. For diazo compound **1**, EDA, complexes **23** and **24** were found. These are structurally similar to complexes **19** and **20**. Complex **24** has a relative energy of −13.1 kcal/mol and is consequently lower in energy than complex **12** (−12.1). Complex **23**, with its energy of −9.4, is less stable, as are styrene−catalyst complexes **21** and **22**. Taking these results into account, the corrected energy barrier for loss of nitrogen in the EDA system is 15.8 kcal/mol. This is in relatively good agreement with the experimental $\Delta H^{\ddagger}$ value of 15.0 kcal/mol found by Anciaux et al. for carbenoid generation from **1** and $Rh_2(OAc)_4$.[43]

Even though the new 12.7 kcal/mol barrier for nitrogen extrusion in the bromodiazoacetate system is higher than the one initially calculated, the rate-limiting energy barrier for nitrogen loss in cyclopropanations with **2** is still substantially lower than the corresponding barriers for both **1** and methyl vinyldiazoacetate.[18] This rationalizes the results from the rate measurements for cyclopropanation of styrene with **1** and **2**, the lower rate limiting energy barrier resulting in a higher rate for the cyclopropanation with **2** than with **1**. Although complex **5** is higher in relative energy than complex **12**, the overall initial energies of the two systems are largely the same when bystander complexes **20** and **24** are taken into account. The lower energy barrier for nitrogen extrusion in the bromodiazoacetate system is therefore a consequence solely of the fact that the transition state for nitrogen extrusion in this system (**TS-6**) is lower in relative energy than the transition state in the EDA system (**13**). When comparing transition states **TS-6** and **TS-13**, it is also clear that the nitrogen extrusion has proceeded further in **13** than in **TS-6**: The C−N bond is 1.797 Å (Wiberg bond order 0.56) in **TS-6** and 1.930 Å (bond order 0.43) in **TS-13**, an observation that is indicative of an earlier, less product-like transition state in the case of the halogenated diazo compound.

While the formation of carbenoid complex **14** from precursor complex **12** is highly endothermic, the formation of brominated analogue **7** from **5** is a markedly exothermic reaction. Although structurally similar, **7** and **14** differ widely in relative energy: Carbenoid complex **7** has a predicted energy of −16.4 kcal/mol relative to **2** and $Rh_2(O_2CH)_4$, whereas **14** has a relative energy of −1.8 kcal/mol relative to its starting materials. It is evident that the bromine substituent stabilizes the carbenoid complex relative to the diazo compound. The formation of alkenes, formally carbenoid dimers, is a common side reaction in many metal-catalyzed reactions with diazo compounds, and is believed to involve the carbenoid.[10] The experimental observation that hardly any dimerization products are formed in cyclopropanation reactions with **2**, contrasting the reactions with **1**, is also indicative of a higher stability of **7** than of **14**.

For the cyclopropanation step in Rh(II)-catalyzed cyclopropanation reactions with diazocarbonyl compounds, different trajectories of the alkene toward the carbenoid complex have been proposed. Previously, the prevalent belief was that the alkene approaches the carbenoid in a side-on manner.[35] Lately, however, theoretical calculations have supported an end-on approach in which steric interactions between the carbenoid

(43) Anciaux, A. J.; Hubert, A. J.; Noels, A. F.; Petiniot, N.; Teyssie, P. *J. Org. Chem.* **1980**, *45*, 695.

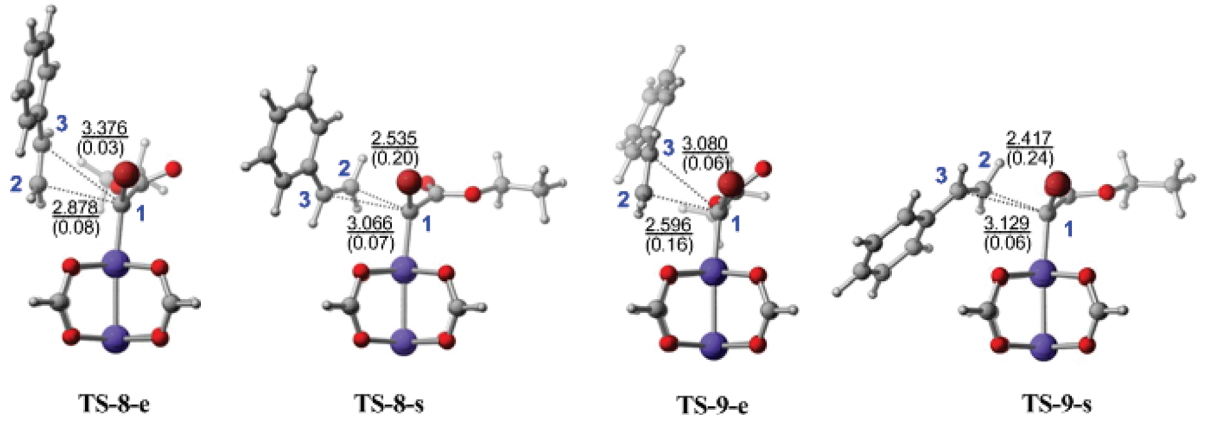

FIGURE 5. Transition states for $Rh_2(O_2CH)_4$-catalyzed cyclopropanation of styrene with ethyl bromodiazoacetate (**2**). Numbering of carbon atoms in blue, C1−C2 and C1−C3 bond lengths underlined, bond orders in parentheses.

ester group and substituents on the alkene are minimized.[18,22,40] Our results show that an end-on approach of the alkene is indeed favored in the case of cyclopropanation of styrene with **2**. Of the two end-on trajectory transition states **TS-8-e** and **TS-9-e**, transition state **TS-8-e**, which leads to *Z*-substituted cyclopropane **10**, is the more favored. In this transition state, styrene approaches the carbenoid complex with the phenyl ring *syn* to the bromine atom, avoiding steric interactions with the ester group. The predicted Rh−C···C=C dihedral angle is −174.4°, and the carbonyl is tilted away from styrene, with a Rh−C−C=O dihedral angle of −107.1°. In transition state **TS-9-e**, which leads to cyclopropane **11**, styrene approaches with the phenyl ring *syn* to the ester group, and the carbonyl is once again tilted away from styrene. Both **TS-8-e** and **TS-9-e** represent small energy barriers, of 0.7 and 1.8 kcal/mol respectively. Transition states in which the carbonyl is tilted toward styrene were also identified in both cases, only 0.1 kcal/mol higher in energy than **TS-8-e** and **TS-9-e**. But even though the transition states with an end-on approach by the alkene are the most favored, the side-on approach cannot be disregarded: Transition states in which styrene approaches the carbenoid through a side-on trajectory were also identified. Side-on trajectory transition state **TS-9-s** represents a barrier of 4.9 kcal/mol and is not of importance, but **TS-8-s** represents a barrier of only 2.0 kcal/mol. In this transition state the predicted Rh−C···C=C dihedral angle is 71.4°. The carbonyl is tilted toward the incoming styrene, the isomer with the carbonyl tilted away disfavored by 0.4 kcal/mol.

Though concerted, the cyclopropanation step is asynchronous, with bond formation between the carbenoid carbon (C1, Figure 5) and the terminal olefinic carbon (C2) happening slightly ahead of bond formation between the carbenoid carbon and the internal olefinic carbon (C3). The most favored transition state, **TS-8-e**, is predicted to be slightly more asynchronous than the other end-on trajectory transition state (**TS-9-e**); the difference between the C1−C3 and C1−C2 distances is slightly larger in **TS-8-e** than in **TS-9-e**. Styrene is also farther away from the carbenoid in **TS-8-e** than in **TS-9-e**, and the C1−C2 and C1−C3 bond orders are lower, indicating that the lower energy transition state **TS-8-e** is earlier than **TS-9-e**. Side-on trajectory transition state **TS-8-s** is later than both **TS-8-e** and **TS-9-e** and also more asynchronous. Transition state **TS-9-s** is considerably higher in energy than the three others, most likely disfavored by the close proximity of the styrene phenyl ring to the formate ligands, and it is more asynchronous than the others. In all four of the transition states the C1−C2 and C1−C3 bond orders are low. This is indicative of early, reactant-like transition states for the cyclopropanation step.

The transition states found for cyclopropanation with EDA (**1**), transition states TS-**15-e**, TS-**15-s**, and **TS-16-e**, are shown in Figure 6. The transition states for cyclopropanation with **1** are all, by varying degrees, earlier than the corresponding transition states for cyclopropanation with **2**. This is evident from the C1−C2 and C1−C3 bond orders and bond lengths and is also reflected in their structures: Nearly no rehybridization of the carbenoid carbon from sp_2 to sp_3 has taken place, as seen by the angle between the carbenoid substituents. **TS-16-e**, the transition state leading to the least stable of the two cyclopropanes (**18**), is the most stable of the transition states, and also, based on bond orders, the earliest. Of the two transition states leading to cyclopropane **17**, the side-on trajectory transition state is lower in energy than the end-on trajectory transition state and also more asynchronous. In the EDA system, we were not able to locate a side-on trajectory transition state similar to **TS-15-s** leading to cyclopropane **18** nor any transition states with the ester carbonyl tilted away from the incoming styrene. Nowlan et al. have previously postulated extremely early, barrierless transition states for cyclopropanation with methyl diazoacetate,[18] and we do not exclude the possibility that other, earlier transition states than the ones we located, may exist. However, if the diastereomeric ratio is calculated based on transition states **TS-15-e**, **TS-15-s**, and **TS-16-e**, the result is 1.2:1, which corresponds nicely with the reported 1.6:1.[10]

The cyclopropanation step in reactions with both the diazo compounds **1** and **2** is highly exothermic, and the transition states are expected to be very early. Nonetheless, the transition states for cyclopropanation with **2** are significantly later than those with **1**, thus making steric interactions more important, as illustrated by the inability of **2** to react with the stilbenes.[15] This sets **2** apart from **1** in cyclopropanation reactions by enabling reactions of higher selectivity and is the basis for the observed diastereoselectivity of the cyclopropanations with **2**. The energetic distribution of end-on and side-on transition states leading to the two diastereomeric cyclopropanes **10** and **11** corresponds, by the Boltzmann equation, to a diastereomeric ratio of 6.9:1, favoring **10**. This is in rather good agreement with the experimentally determined diastereomeric ratio of 9:1.[15]

The NBO charge distribution during the reaction course reveals additional information about the cyclopropanation reaction. As complex **5** between diazo compound **2** and $Rh_2(O_2CH)_4$ is formed, negative charge moves from the diazo compound into the catalyst part of the complex, rendering the diazo ligand with a predicted overall charge of +0.17 and consequently the catalyst with an overall charge of −0.17. In the nitrogen extrusion step (**TS-6**) more negative charge moves into the $Rh_2(O_2CH)_4$ part of the complex, which now has an

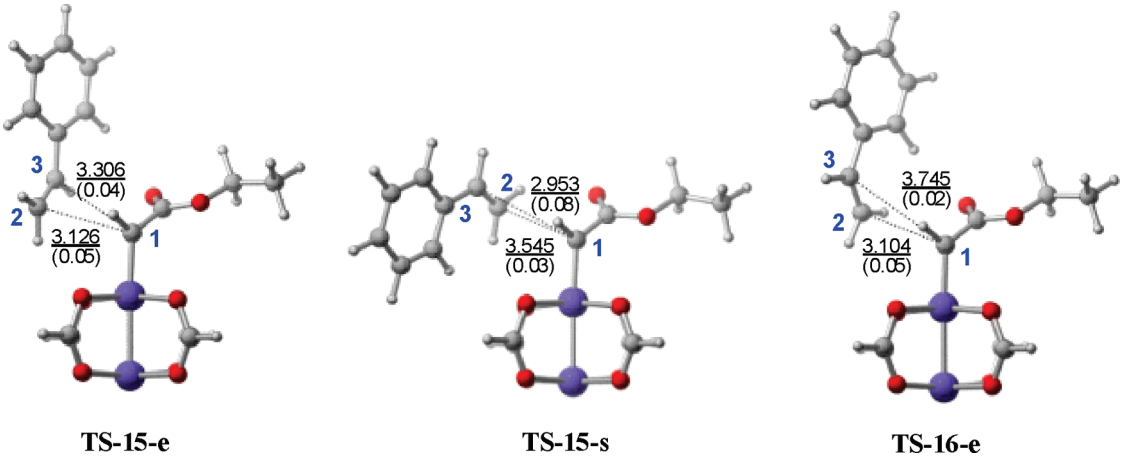

FIGURE 6. Transition states for $Rh_2(O_2CH)_4$-catalyzed cyclopropanation of styrene with EDA (**1**). Numbering of carbon atoms in blue, C1−C2 and C1−C3 bond lengths underlined, bond orders in parentheses.

overall negative charge of −0.21. The separation of charge is somewhat less pronounced in carbenoid complex **7**, where the $Rh_2(O_2CH)_4$-part of the complex has an overall charge of −0.15. The +0.15 charge on the carbenoid ligand indicates an electrophilic carbenoid, and this is supported by the considerable contribution of the $2p_z$ orbital of the carbenoid carbon in the LUMO of the carbenoid complex (Figure 7). A significant contribution is also made by the bromine p_z orbital. A similar trend regarding charge distribution is seen with EDA (**1**), with a predicted charge of +0.18 on the diazo ligand in complex **12**, +0.24 (including N_2) in **13**, and +0.16 on the carbenoid ligand in complex **14**. The $2p_z$ orbital of the carbenoid carbon once again contributing considerably to the LUMO of the carbenoid complex, confirms that this is also an electrophilic carbenoid.

The four transition states **TS-8-e**, **TS-8-s**, **TS-9-e**, and **TS-9-s** for cyclopropanation with brominated carbenoid **7** all differ from each other in the charge distributions. In the most favored transition state, end-on trajectory transition state **TS-8-e**, the catalyst part of the complex has a total charge of −0.20, while styrene and the carbenoid ligand both have charges of +0.10. In the higher energy end-on trajectory transition state **TS-9-e**, there is higher charge buildup on the carbenoid: The catalyst has a total charge of −0.21, but styrene is considerably more positive than in **TS-8-e**, with a charge of +0.18, and the carbenoid is correspondingly less positive, +0.03. As **TS-8-e** and **TS-9-e** are both very early transition states, and **TS-8-e** earlier than **TS-9-e**, these results paint a picture of a cyclopropanation step in which charge transfer from the olefin to the carbenoid precedes charge transfer in the opposite direction, even though the transformation follows a concerted mechanism. In the side-on trajectory transition states, **TS-8-s** and **TS-9-s**, styrene has a charge of +0.24 and +0.26, respectively.

Cyclopropanation of Styrene with Ethyl Chlorodiazoacetate (3) and Ethyl Iododiazoacetate (4). Figure 8 shows the energy profiles of the reaction courses for $Rh_2(O_2CH)_4$-catalyzed cyclopropanation of styrene with ethyl chlorodiazoacetate (**3**) and ethyl iodiazoacetate (**4**). The energy profiles for **3** and **4** largely mirror the energy profile for **2**, the structures in the reaction with **4** slightly higher in relative energy compared to the corresponding starting materials, and **3** slightly lower. The structures in the reaction pathway for **3** are very similar to the analogous structures for **2**, but there are some differences in the case of **4**, presumably because of the size of the iodine substituent. The carbenoid complex **7-I**, formed from **4** and $Rh_2(O_2CH)_4$, differs from **7** and **7-Cl** in that the most stable rotamer does not have the halogen atom nearly eclipsed to one of the formate ligands, like for **7** and **7-Cl**. Instead, there are two other rotamers, one with

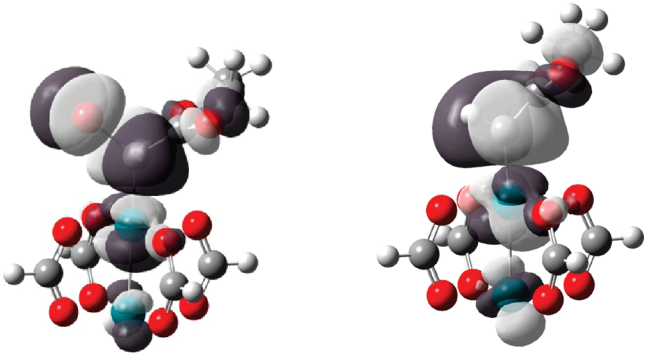

FIGURE 7. LUMO of carbenoid complexes **7** (left) and **14** (right).

iodine and two ligands completely staggered, and one with the iodine slightly closer to one of the formate ligands, that both are 0.1 kcal/mol lower in energy. As expected, the calculated charge distributions show that both the iodinated and the chlorinated carbenoids are electrophilic carbenoids, with a +0.16 charge on the carbenoid ligand in complex **7-Cl** and +0.17 in complex **7-I**.

Both end-on and side-on trajectory transition states were found for cyclopropanation of styrene with the chlorinated and iodinated carbenoids. Their structures largely mirror the transition states found for the brominated analogue, except that the most favored end-on trajectory transition state for the iodinated system has the carbonyl tilted toward styrene (favored by 0.2 kcal/mol), and the most favored side-on trajectory transition state for the chlorinated system has the carbonyl tilted away from styrene (favored by 0.1 kcal/mol). However, the relative stabilities of the side-on and end-on trajectory transition states change with the halogen. While the most stable side-on trajectory transition state in the brominated system, **TS-8-s**, is 0.3 kcal/mol higher in energy than the least stable of the end-on trajectory transition states (**TS-9-e**), the energy difference between chlorinated analogues **TS-8-s-Cl** and **TS-9-e-Cl** is 0.7 kcal/mol. In the iodinated system, the order of these two transition states is reversed: **TS-8-s-I** is 0.3 kcal/mol more stable than **TS-9-e-I**, so that both of the transition states leading to *Z*-substituted cyclopropane **10-I** are more favored than the lowest energy end-on transition state leading to *E*-substituted cyclopropane **11-I**. In the cyclopropanation reaction with **3** the side-on trajectory transition state leading to *E*-substituted cyclopropane **11-Cl** is considerably higher in energy than the other transition states, paralleling the results with **2**, and thus

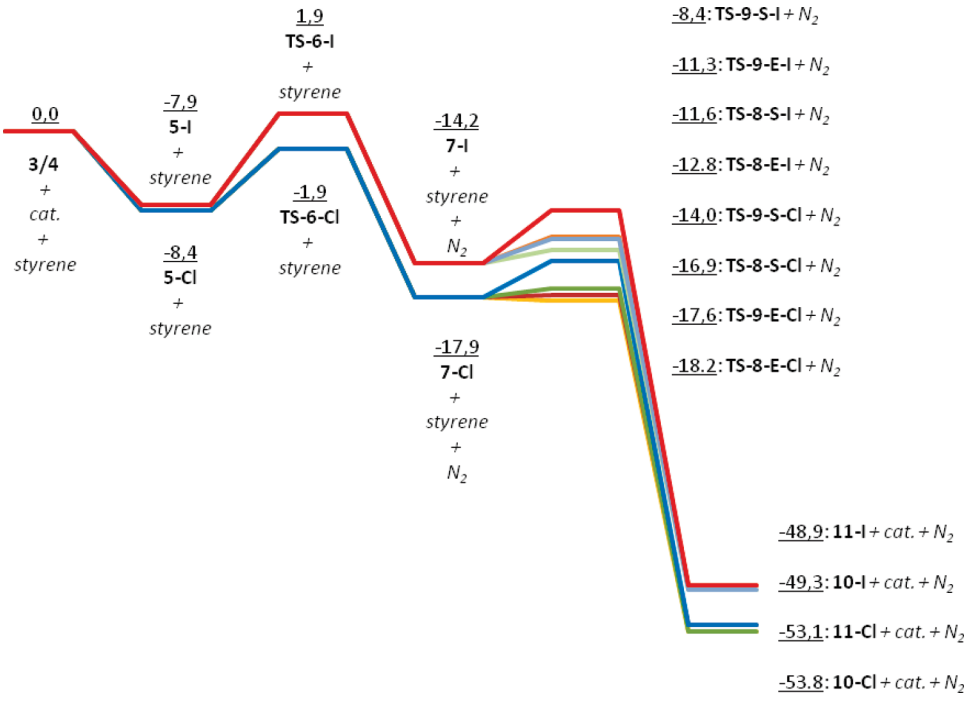

FIGURE 8. Energy profile for $Rh_2(O_2CH)_4$-catalyzed cyclopropanation of styrene with ethyl chlorodiazoacetate (**3**) and ethyl iododiazoacetate (**4**).

TABLE 1. Diastereomeric Ratios for Halogenated Cyclopropanes

diazo compound	calcd dr	experimentally determined dr[15]
ethyl diazochloroacetate (**3**)	3.5:1	6:1
ethyl diazobromoacetate (**2**)	6.9:1	9:1
ethyl diazoiodoacetate (**4**)	11.9:1	14:1[a]

[a]Closer inspection of crude ^{1}H-NMR data gives this dr, rather than the previously reported 9:1.

not of importance, but in reaction with **4**, transition state **TS-9-s-I** is only 2.7 kcal/mol higher in energy than **TS-8-s-I**.

For cyclopropanation with the chlorinated carbenoid complex, transition state **TS-8-e-Cl** is slightly lower in energy than precursors **7-Cl** and styrene, −0.3 kcal/mol, while **TS-9-e-Cl** and **TS-8-s-Cl** represents barriers of 0.2 and 1.0 kcal/mol. For the iodinated analogue, all four important transition states are predicted to be potential energy barriers, of 1.5, 2.6, 2.9, and 5.3 kcal/mol respectively. Table 1 shows the diastereomeric ratios calculated using the Boltzmann equation along with the experimentally determined[15] diastereomeric ratios for all three halogenated systems.

The calculated diastereomeric ratios correspond well with the experimental results, predicting a higher diastereomeric ratio for the iodinated than for the brominated cyclopropanes and a lower diastereomeric ratio for the chlorinated analogs.

Side-on versus End-on Model. It is evident from our results that in the $Rh_2(O_2CH)_4$-catalyzed cyclopropanation of styrene with halodiazoacetates the halogen substituents influence the relative energies of the different trajectories of styrene toward the carbenoid. The energy barriers represented by each of the lowest-energy end-on and side-on trajectory cyclopropanation transition states are higher in the iodinated system than in the brominated system and lower in the chlorinated system (Figure 9). This observation is most likely explained by the size of the halogen substituent; the more sterically demanding the halogen, the higher the energy of each transition state.

However, the increase in relative energy on going from chlorine to bromine to iodine is slightly less for the most favored

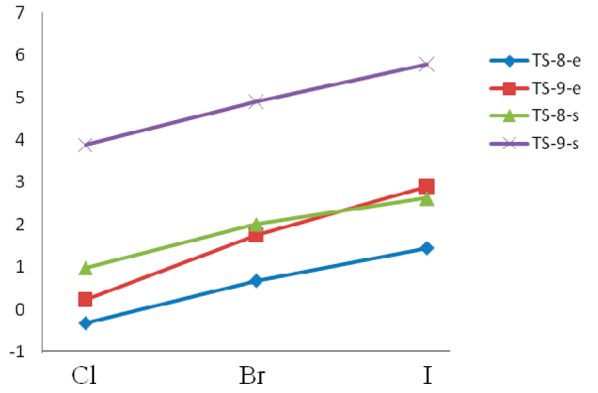

FIGURE 9. Transition-state energy, relative to corresponding precursor carbenoid complex, as a function of halogen substituent.

of the side-on trajectory transition states (**TS-8-s**), than for the three other transition states, meaning that the increasing size of the halogens have less of a negative effect on this transition state. This may be rationalized by certain molecular orbitals: In the **TS-8-s** transition states in the iodinated and brominated systems, there are molecular orbitals that show direct interaction between the halogen and the π-system of the styrene phenyl ring, not involving the alkene. An example is shown in Figure 10. The larger iodine substituent was found to overlap better with the phenyl π-system than does bromine, resulting in additional molecular orbitals showing halogen−phenyl interactions in the iodinated system compared to the brominated. Direct interactions between the phenyl group and the halogen in the case of the smaller, more electrophilic chlorine were not identified. This may explain why the side-on trajectory transition states are more favored relative to the end-on trajectory transition states in the iodinated system, and less in the chlorinated.

The substituents on the carbenoid carbon are not the only factor that affects the relative stability of the different cyclopropanation transition states: The search for transition states

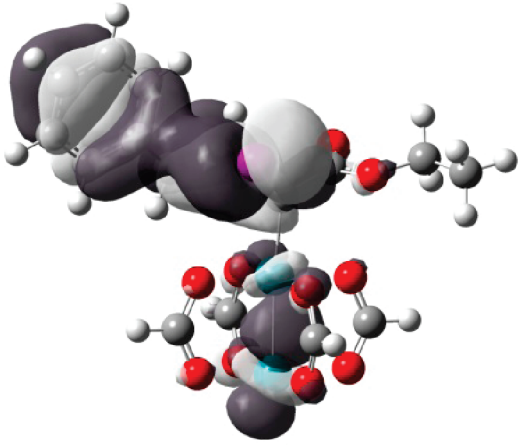

FIGURE 10. HOMO-4 orbital of transition state **TS-8-s-I** (carbenoid complex in the front, styrene back left).

for the cyclopropanation of *N*-vinylphthalimide with bromodiazoacetate **2** gave interesting results. In this reaction, the side-on trajectory transition state (**TS-25-s**, Figure 11) leading to the *Z*-substituted, most stable cyclopropane is lower in energy than both of the most stable end-on transition states (**TS-25-e** and **TS-26-e**): While **TS-25-e** and **TS-26-e** represents calculated barriers of 1.5 and 2.3 kcal/mol, respectively, **TS-25-s** represents a barrier of 1.4 kcal/mol relative to precursor carbenoid complex **7**. As in the cyclopropanation with styrene, the side-on trajectory transition state (**TS-26-s**) leading to the *E*-substituted cyclopropane is much higher in energy than the others.

The transition states in this reaction are structurally similar to those in the cyclopropanation of styrene, but with the alkene somewhat more tilted relative to the C−Rh-axis. All but **TS-25-e** also have the carbonyl tilted in the opposite direction to what is preferred in the analogous transition states with styrene, but with the other rotamer only slightly higher in energy (0.1−0.3 kcal/mol). Bond orders show that **TS-25-s** and **TS-26-e** are approximately as early and as asynchronous as their styrene-counterparts **TS-8-s**, **TS-9-e**, and **TS-9-s**, but **TS-25-e** and **TS-26-s** are later and more asynchronous than **TS-8-e** and **TS-9-s**. Taking all favored transition states into account, the calculated diastereomeric ratio, using the Boltzmann equation is 11.2:1. This is substantially higher than the calculated diastereomeric ratio for cyclopropanation of styrene with the same diazo compound (**2**), in correspondence with the experimentally determined results.

The existence of low energy side-on trajectory transition states has consequences for the use of models to rationalize the stereochemical outcome of carbenoid cyclopropanation reactions. Even though the end-on model satisfactorily explains the origin of the observed diastereoselectivity in certain carbenoid cyclopropanations with styrene,[18] our results show that this model cannot be used exclusively in all instances, as side-on trajectory transition states also can be important. We have found that the relative energies of side-on versus end-on trajectory transition states can be governed by both the substrate alkene and the substituents on the carbenoid carbon. The prospect that other factors, such as the choice of catalyst, also may have an influence cannot be ruled out. The possible existence of more than one favored type of transition state should thus be taken into consideration when using models to explain or predict diastereo- and enantioselectivity in carbenoid cyclopropanation reactions.

Stabilized Carbenoids. The classification of Rh(II) carbenoids as acceptor-, donor/acceptor-, or acceptor/acceptor-substituted carbenoids is frequently encountered. The substituents on the carbenoid carbon are divided into either donors or acceptors, while hydrogen is neither nor. As halogens can potentially act as σ-acceptors, π-donors, or both, a closer look at the halogenated carbenoids is in its place. Carbenoid complex **14**, generated from EDA, is a natural point of comparison. In this complex, the carbenoid C−H bond is a σ-bond with bond order 0.91. The hydrogen substituent, being a σ-donor, has a predicted NBO charge of +0.23. The carbenoid carbon has a charge of −0.11, which may sound counterintuitive as the carbenoid reacts as an electrophile. However, as Sheehan et al. note,[24] ground-state atomic charge is not necessarily a predictor of reactivity, and the electrophilic reactions of negatively charged carbenoids can be nicely explained by assuming initial interactions of the nucleophile with the carbenoid resulting in redistribution of the electrons in the carbenoid complex.

Inspection of the orbitals of carbenoid complex **7** sheds light on the halogens' effect on a carbenoid; molecular orbitals can be identified in which a bromine p-orbital clearly is interacting with the orbital making up the π-component of the C−Rh bond, as exemplified by HOMO-22 (Figure 12). This indicates that the p_z-orbital of the carbenoid carbon is subject to not only back-donation from the vicinal rhodium atom but also donation of electron density from bromine. The NBO charges confirm that the bromine−carbon interaction indeed has bromine acting as an

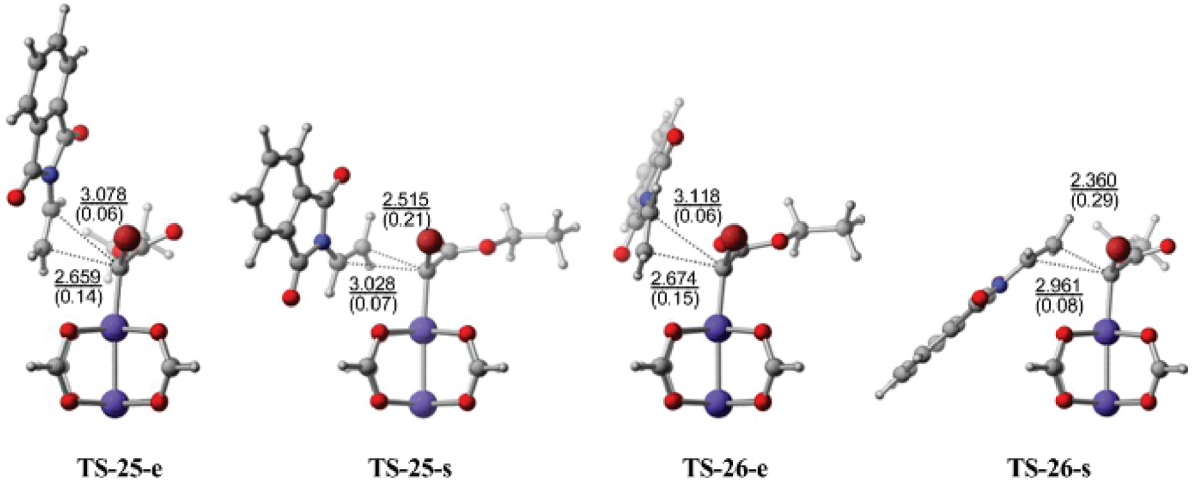

FIGURE 11. Transition states for $Rh_2(O_2CH)_4$-catalyzed cyclopropanation of *N*-vinylphthalimide with ethyl bromodiazoacetate (**2**). Underlined numbers refer to carbon−carbon bond lengths; numbers in parentheses refer to bond orders.

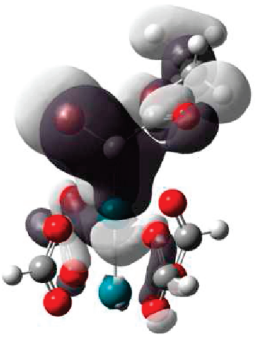

FIGURE 12. HOMO-22 orbital of carbenoid complex **7**.

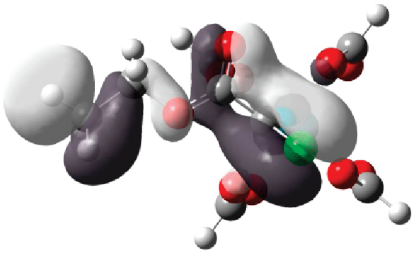

FIGURE 13. HOMO-25 orbital of carbenoid complex **7-Cl** (viewed down the C−Rh−Rh axis).

electron donor; the bromine atom in complex **7** has a predicted positive charge of +0.24, while the charge on the carbenoid carbon is −0.15. The relatively short 1.860 Å C−Br bond in **7**, reflected in a bond order of 1.29, can also be seen as a manifestation of the partial C−Br π-bond.

Both the iodine and chlorine substituents display π-interactions with the carbenoid carbon in the same fashion as bromine; orbitals with a Rh−C-halogen π-electron cloud similar to the one in Figure 12 can be identified for complexes **7-Cl** and **7-I**. The halogen−carbon bond orders of 1.31 in **7-Cl** and 1.27 in **7-I** are also close to the bond order in **7**. NBO analyses reveal that the electronegative chlorine in complex **7-Cl** as well as the iodine in complex **7-I** are positively charged and that the carbenoid carbons are negatively charged. The magnitude of the charges changes with the halogen, the iodine bearing a charge of +0.35, and the chlorine +0.17. The magnitude of the negative charge on the carbenoid carbon varies correspondingly, −0.07 in **7-Cl** and −0.24 in **7-I**. The analogous fluorinated carbenoid complex (not shown) has yet to be synthesized, but its calculated properties are informative. In this complex the predicted charges on fluorine and the carbenoid carbon are −0.27 and +0.44, respectively, the C−F bond order is 1.04, and no orbitals can be identified that indicate π-donation from fluorine into the C−Rh π-bond. It seems clear from these results that fluorine must be a pure σ-acceptor and, consequently, that the charge on the carbenoid carbon can be strongly affected by σ-acceptors. Therefore, any inductive σ-accepting effects of the other halogens on the carbenoid carbon, likely by the Pauling electronegativity scale at least in the case of chlorine and bromine, cannot be ruled out. It is nevertheless evident from the positive charge on the halogens that if any of the halogens indeed are electron-withdrawing inductively, this effect is outweighed by electron donation through the π-system.

In conclusion, the halogen substituents in carbenoid complexes **7**, **7-Cl**, and **7-I** are all undeniably "donors", donating electron density toward the C−Rh π-bond through resonance, and in the case of chlorine and bromine most likely also "acceptors", accepting electron density inductively through the halogen-carbon σ-bond. In order to place the halogenated carbenoids into the standard categories, as either acceptor-, donor/acceptor- or acceptor/acceptor-substituted carbenoids, the most practical way is to overlook this ambiguity and consider the charge on the halogen substituents. With hydrogen as the zero-point of the scale, this means that iodine is a net donor substituent, chlorine is an acceptor, and bromine a very weak donor. Hence, **7-I** is a donor/acceptor-substituted carbenoid, **7** is an acceptor-substituted carbenoid, and **7-Cl** is an acceptor/acceptor-substituted carbenoid. The perhaps most informative description of carbenoids **7**, **7-Cl**, and **7-I**, however, is as *stabilized* carbenoids. The stabilizing effect of the halogens on the carbenoids is evident from the higher stability of **7**, **7-Cl**, and **7-I** compared to hydrogen-substituted carbenoid **14**, as shown by their low tendency to dimerize, and might be a consequence of the π-interaction between the halogen and the C−Rh bond. The stability of **7**, **7-Cl**, and **7-I** affects the position of their transition states in cyclopropanations: Still early, the transition states for cyclopropanation with the halogenated carbenoids are later than the transition states with **1**, and contrasting transition states **TS-15-e**, TS-**15-s**, and **TS-16-e**, the transition states in the halogenated systems all represent potential energy barriers. This can make electronic interactions between the carbenoid and the alkene substantially more important in the cyclopropanations with the halogenated carbenoids, and might explain why **7-I**, with the larger, less electronegative iodine substituent, gives a higher diastereomeric ratio than **7** and why the diastereomeric ratio with **7-Cl** is lower.

A notable structural feature of all the halogenated carbenoid complexes, **7**, **7-Cl**, and **7-I**, is that the ester carbonyl is almost perpendicular to the C−Rh bond, meaning that the carbonyl π-orbital and the C−Rh π-orbital are not in conjugation with each other. The Rh−C−C=O dihedral angle in the halogen-containing complexes ranges from −93.9° in complex **7-Cl**, via −89.7° in **7**, to −85.7° in complex **7-I**. In complex **14**, formed from EDA (**1**), the angle is −106.5°. Previously, the carbonyl π-orbital and the C−Rh π-orbital were assumed to be parallel in all carbonyl-substituted dirhodium−carbenoid complexes, favorably aligned for conjugation, but computational studies have lately shown that this is not the case. In all the studied complexes the carbonyl is twisted out of conjugation with the C−Rh bond, but the reasons behind this unexpected conformation are not yet fully understood. Nowlan et al. propose that the twisted conformation of the carbonyl in methyl vinyldiazoacetate results in a favorable alignment of the carbonyl π*- with the C−Rh π-orbital,[18] while Nakamura et al. have identified orbitals that show how the positioning of the carbonyl in methyl diazoacetate enables interactions between the carbonyl π-bond and the C−Rh σ-bond.[21] Examination of the occupied orbitals in complexes **7**, **7-Cl**, **7-I**, and **14** confirm that in these complexes, too, there are molecular orbitals that result from carbonyl π-orbitals interacting with C−Rh σ-orbitals because of the twisted position of the carbonyl. For the halogenated carbenoid complexes additional interactions involving the ester carbonyl are of importance. For **7** and **7-I**, a lone pair from the carbonyl oxygen interacts with the π-electron cloud made up from the C−Br and C−Rh π-bonds, as shown for **7** in Figure 12. For **7-Cl** (Figure 13) no involvement of the lone pairs can be identified. Instead, there seems to be an interaction between a carbonyl π-orbital and the Rh−C−Br π-electron cloud, similar to Nowlan et al.'s suggestion for methyl vinyldiazoacetate.

No interaction between the carbonyl and the C−Rh π-bond can be seen in complex **14**. The additional π-interactions involving the carbonyl can explain the somewhat different Rh−C−C=O dihedral angle in the halogenated carbenoid complexes compared to others and might represent an additional stabilizing factor in these complexes.

Conclusions

In this paper, we have presented a full computational study of the reaction mechanism for $Rh_2(O_2CH)_4$-catalyzed cyclopropanation with ethyl halodiazoacetates **2**−**4**. The high kinetic activity of the halodiazoacetates has been explained by the computational results, which show that the energy barrier of the rate limiting step, nitrogen extrusion from the catalyst-coordinated diazo compound, is substantially lower for the halodiazoacetates than for other studied diazo compounds. Experimental results show a low tendency for dimerization in reactions with the halodiazoacetates, indicating a relatively stable carbenoid. This, too, has been confirmed computationally: The carbenoid formation is markedly exothermic, with the carbenoid much more stable than the corresponding diazo compound and catalyst. Examination of the molecular orbitals of the halogenated carbenoids shows interactions between the halogen $2p_z$-orbital and the π-component of the carbon−rhodium bond, resulting in a delocalized π-electron cloud extending from rhodium via the carbenoid carbon to the halogen, a phenomenon that might be the basis for the observed stability. By the traditional classification of carbenoids, iodinated carbenoid **7-I** is a donor/acceptor-substituted carbenoid, brominated analog **7** is an acceptor-substituted carbenoid, while the chlorinated analogue, **7-Cl**, is an acceptor/acceptor-substituted carbenoid. They are all three stable enough that the transition states for their cyclopropanation of styrene represent potential energy barriers, whose heights are likely to be governed by the size of the halogen, leading to an excess of one of the two diastereomeric cyclopropane products. Contrasting previous computational studies of other diazo compounds,[18,22,39,40] cyclopropanation transition states with a side-on as well as an end-on trajectory of the styrene toward the carbene were found to be of importance in the case of the halodiazoacetates. The stability of the side-on trajectory transition states relative to the end-on trajectory transition states was shown to depend both on the halogen and the substrate olefin; the side-on trajectory transition states are more favored in the cyclopropanation of styrene with iododiazoacetate **4** than with bromodiazoacetate **3** and less with chlorodiazoacetate **2**, and they were more favored in reaction with *N*-vinylphthalimide than with styrene. In all cases, the predicted diastereomeric ratio of the reactions corresponds well with the experimental results. The fact that both side-on and end-on trajectory transition states can be of varying importance depending on the alkene as well as the diazo compound is something that should be taken into consideration when using models to explain and predict the stereochemical outcome of cyclopropanation reactions and in the rational design of new catalysts for these reactions.

Acknowledgment. We thank Jens H. F. Aasheim and Dr. Andreas Krapp for technical support.

Supporting Information Available: Energies and full geometries for all structures. This material is available free of charge via the Internet at http://pubs.acs.org.